

MEASUREMENT RECEIVER ERROR ANALYSIS FOR RAPIDLY VARYING INPUT SIGNALS

O. M. Caldwell

Scientific-Atlanta Inc.
3845 Pleasantdale Rd.
Atlanta, GA. 30340

ABSTRACT

An assessment of instrumentation error sources and their respective contributions to overall accuracy is essential for optimizing an electromagnetic field measurement system.

This study quantifies the effects of measurement receiver signal processing and the relationship to its transient response when performing measurements on rapidly varying input signals. These signals can be encountered from electronically steered phased arrays, from switched front end receive RF multiplexers, from rapid mechanical scanning, or from dual polarization switched source antennas.

Numerical error models are presented with examples of accuracy degradation versus input signal dynamics and the type of receiver IF processing system that is used. Simulations of far field data show the effects on amplitude patterns for differing rate of change input conditions. Criteria are suggested which can establish a figure of merit for receivers measuring input signals with large time rates of change.

Key Words: Antenna Measurements, Measurement Accuracy, Discrete Time Signal Processing

1.0 INTRODUCTION

The effects of measurement receiver bandwidth when performing measurements on rapidly varying input signals can be a source of errors in electromagnetic field measurements. Rapidly varying test signals are commonly encountered when measuring electronically steered phased arrays due to their fast beam switching. Time division multiplexing techniques used for multi-channel applications, switched dual polarization source antennas for co and cross polarized measurements, and even rapid mechanical scanning of single beam antennas also produce signals with large time rates of change.

One of the historical figures of merit for measurement receiver dynamic performance has been pre-detection IF bandwidth. This design parameter has traditionally been the major factor in determining both the final noise figure of the receiver and its transient response. A fundamental problem for traditional signal processing topologies has been how to preserve system noise figure while improving transient response in the pre-detection stages. This is important since the linear dynamic range depends on both the peak signal at a given compression point and the minimum detectable signal, or noise floor, which is equal to kTB (k is Boltzman's constant, T is temperature, and B is bandwidth). Unless the maximum linearly detected signal can be increased, B is the only parameter that can be easily manipulated to improve dynamic range.

However, new circuit and signal processing topologies for precision microwave instrumentation allow the coupled nature of the bandwidth and transient response parameters to be significantly reduced. Therefore, the fundamental basis for the simple comparison of receiver bandwidths to predict both performance parameters is no longer necessarily valid. This paper will compare the dynamic performance of traditional receiver topologies and signal processing with that of a new baseband signal processing technique utilized in the Scientific-Atlanta Model 1795. A comparison of measurement precision for typical antenna patterns will be evaluated for both classes of topologies, characterized by network models.

2.0 MEASUREMENT RECEIVER DETECTION THEORY AND PRACTICE

2.1 BACKGROUND

The signal processing analysis of precision microwave measurement instrumentation is predicated on utilizing the theory of causal, linear, time invariant networks. Such linear networks can be further classified into the general categories of instantaneous or dynamic networks. Instantaneous networks are simply those whose outputs at any instant in time are dependent only on the inputs presented to the network at that same instant. In a theoretical sense, these networks have infinite bandwidth and cannot be physically realized. Even so, simplifying assumptions are often used when bandwidths of some system elements are orders of magnitude greater than other elements. Conversely, dynamic networks have the property that their outputs are dependent not only on the present state of the inputs at any instant of time, but on the previous values of these inputs as well. A network whose output at time t is completely determined by the inputs presented in the previous interval $t-T$, is defined to have a memory of length T (4). When processing signals in the continuous time domain, T is theoretically infinite, although some finite value for it is easily obtained for a given level of error in the outputs. Signal processing techniques in the discrete time domain can set T to a controllable and finite value. This feature of discrete time processing is very useful since digital signal processing and microprocessor based architectures are universally used in modern instrumentation. This memory length has a significant effect on measurement precision when rapidly varying input signals are applied to a dynamic network. The effects can be evaluated by computing the time domain convolution integral based on the characteristics of modern instrumentation and simulated excitation functions.

2.2 MEASUREMENT RECEIVER SIGNAL PROCESSING

Figure 1 shows a block diagram of the signal processing of a typical measurement receiver. A switched input signal is also shown to portray time division multiplexed operation for multi-channel capability. The basic architecture utilizes a dual downconversion technique to maximize sensitivity and facilitate phase locking to the excitation (phase locked circuits omitted for clarity). Of particular interest are the bandlimiting filters following the mixers. These filters are vital components in determining the noise figure of the instrument and thus its sensitivity and dynamic range. They also play a major role in

determining the transient response of the instrument, so a tradeoff in sensitivity and the time domain characteristics for such a system design is inevitable.

2.2.1 TIME DOMAIN ANALYSIS

A fundamental aspect of linear system analysis is the convolution theorem. In its simplest form, the theorem states that the output of a linear, time invariant system as a function of time can be uniquely determined by evaluating the convolution integral of its impulse response over all time with the input excitation as a function of time. The familiar equation for convolution is given in Equation 1 where $y(t)$ is the output, $h(t)$ is the impulse response and $x(\tau)$ is the excitation. τ is the dummy variable of integration (2).

$$y(t) = \int_0^t x(\tau) h(t-\tau) d\tau \quad (1)$$

If the impulse response of a circuit can be accurately measured or estimated, then its response can be known for an arbitrary input signal. Since this is a time domain calculation, the results of such computations can characterize the transient response of linear networks without invoking the Laplace transform or solving high order differential equations. Fortunately, estimation of the impulse responses of the filters used in the IF and baseband circuits of measurement receivers is straightforward.

In particular, the lowpass filter functions used in earlier generation receivers and even the present generation of vector network analyzers can be modeled as a single pole passive network as shown in Figure 2. The hi-Q bandpass filters (BPF) used in today's network analyzers at the first IF frequency can be translated to lowpass (LPF) types at the baseband (second IF) frequency to form one composite filter function. In actual practice, these filters are complex and result in time domain responses somewhat slower than the single pole case, but the single pole model can be used as a best possible estimate for response time. The impulse response $h_1(t)$ for this model network is given in Equation 2. The RC time constant sets the 3 dB cutoff frequency of the filter which is directly proportional to its settling time. For these simulations, $RC = 200 \times 10^{-9}$ seconds, which is a good approximation of the time constant used in HP 8510B baseband filter.

$$h_1(t) = \frac{1}{RC} e^{-t/RC} \quad \text{for } t > 0 \quad (2)$$

A more interesting baseband filter/detector utilizing discrete time processing (DTP) techniques is used in the S-A 1795 Receiver and shown schematically in Figure 3. Its corresponding impulse response $h_2(t)$ for one complete measurement cycle utilizing 200 microseconds of aperture time is shown in Equation 3. The SPST switch is used to reset the network to an initial state after every measurement.

$$h_2(t) = K \quad \text{for } 0 < t < 200 \times 10^{-6} \quad (3)$$

0 otherwise

Careful examination of these two types of impulse responses reveals the following:

1. The nonzero aperture times of both networks will "smear" the input signal as it propagates through the network to the output. The resulting distortion due to this smearing process is inversely proportional to the bandwidth of a continuous time network or directly proportional to the aperture time of the discrete time process.
2. The bounded time extent of the DTP technique will reduce the amount of signal distortion compared to the unbounded time extent of the LPF or BPF impulse responses.
3. The bandwidth of the LPF is inextricably linked to its transient response via the RC time constant. The infinite memory length T of this function as discussed in Section 2.1 is a performance limitation of a continuous time network.
4. The memory length of the DTP technique is fixed simply by the measurement interval. The bandwidth of the DTP technique is proportional to the Fourier transform of the measurement interval. This results in a $\sin(f)/f$ response which theoretically has infinite bandwidth. Therefore, a value for the IF bandwidth of a DTP based receiver is not meaningful. However, the $\sin(f)/f$ response can be integrated to obtain an equivalent noise bandwidth (ENB) which can be useful in noise calculations. The S-A 1795 ENB for one sample is approximately 6600 Hz. The wideband response of the DTP aliases some out of band noise into the baseband region. Since the receiver is operated phase locked to the excitation source, there are no coherent signal components in the out of band spectrum. The only effect is that the overall noise figure of the instrument is degraded a few dB by the noise.

An additional aspect of modern receiver operation is the ability to coherently average multiple measurements to reduce uncertainty due to uncorrelated noise. This technique is quite useful but it increases the signal memory length by a factor of 2 for every 3 dB of integration gain. Depending on the signal rate of change, this can result in actually decreasing measurement precision due to increasing convolutional errors at a faster rate than reducing uncertainty due to noise.

3.0 DATA SIMULATIONS

An appropriate aspect of the relative performance of these network types is how each responds to signals encountered during typical antenna measurements. This section will examine the measurement precision degradation for differing rate of change input conditions on simulated amplitude patterns using these network models.

Note that the error levels in these simulations represent the best possible response conditions for the networks. These errors are independent of the actual sampling rates used since digitization is a separate process from the baseband filtering or detection in either case. The errors given for the DTP technique represent those for 1 sample, equivalent to a 5 KHz continuous data rate.

Example #1

Consider a 2 foot parabolic dish antenna operating at 8 GHz. This antenna has a 3 dB beamwidth of 4.5 degrees, and a first null at 6 degrees from boresight. For an antenna of this size, a scanning rate of 1.0 RPM, or 6 degrees per second is certainly reasonable. The ideal far field copolarized response (in linear units) is described by a $\sin(\theta)/\theta$ response with the pattern shown in Figure 4 for one side of the main lobe. Although this is not a particularly rapidly varying signal, knowing how accurately each network model will track the input signal from the AUT as a function of time is a useful check of the process.

Convolving the impulse responses of the networks with the ideal pattern as a function of time produced the error plots shown in

Figure 5 for the LPF and the DTP technique. These plots show the level in dB of the networks' error below the pattern level. The peak error level of the LPF is -74 dB while the peak error of the DTP technique is -84 dB. Notice that the errors of both networks essentially vanish at the beam peak location since the rate of change of the pattern is 0. The -74 dB error signal corresponds to a pattern measurement error of .0017 dB. The -84 dB error signal corresponds to a pattern measurement error of .00055 dB. These errors are below the level of most range error sources, but note that they are commensurate with the uncertainties due to static dynamic range limitations of modern receivers due to noise (1).

Example #2

Next consider a spinning linearly polarized source antenna commonly used to measure the copolarized and cross polarized response of an AUT. The spinning rate of the source antenna is 10 RPM and the AUT is the same as used in Example #1. The cross-polarization ratio of the source antenna is assumed to be 30 dB. The AUT cross-polarization ratio is large, assumed to be greater than 50 dB. A good approximation of the cross-polarized response for the main lobe region is based on sine function weighting (3). The resulting pattern function of time is shown in Figure 6 and is convolved with the same $h_1(t)$ and $h_2(t)$ as in Example #1. The results of this operation indicate more error than seen in Example #1, as shown in the plots of Figure 7. The LPF network has a peak error of -44 dB below pattern level while the DTP technique contributes a peak error -53 dB. The -44 dB error signal corresponds to a pattern measurement error of .055 dB. This level is twice the peak uncertainty due to static dynamic range limitations for an LPF network based receiver such as the HP 8510B (.027 dB). The total receiver related error in this case is thus .082 dB.

The -53 dB error signal corresponds to a pattern measurement error of .019 dB. This error level is very close to the uncertainty due to dynamic range of the S-A 1795 at -30 dB (.012 dB). The total receiver related error for the S-A 1795 is thus .031 dB.

Error levels could be lowered in both cases by reducing the speed of rotation of the polarization and AUT scan axes.

Example #3

Finally consider a data acquisition where the AUT beam is switched as a function of time. A switching rate of 100 Hz is used so that the full settling interval can be examined for both networks. The amplitude values range from -50 dB to 0 dB and are constant during each 10 millisecond interval. A 100 microsecond beam settling time is assumed. The time domain excitation for 4 beam states is shown in Figure 8. This function is convolved with the same $h_1(t)$ and $h_2(t)$ as in Example #1.

The result of this operation shows a large potential error as a continuous function of time for the LPF network as indicated in Figure 9. Although it is possible to achieve precise results using the continuous time filters, the receiver trigger must be delayed after the beam is switched to allow IF settling within a desired error window. For instance, a settling window of 0.1 dB requires at least an 825 microsecond delay. A settling window of 0.01 dB requires a 1300 microsecond delay. This sets an upper limit on sampling rate for a specified error window.

The DTP technique's errors, also shown in Figure 9, are seen as 100 microsecond pulses located at the switching transient. In this example, no settling delay is required although in practice, one complete interval of 200 microseconds is needed to ensure complete capture of the new level. If synchronization of the measurement interval with the beam switching is allowed, the error will vanish completely since the detector is reset during the beam switching discontinuity.

4.0 PERFORMANCE CRITERIA

Based on the results of these simulations, criteria which produce a figure of merit for receivers measuring input signals with large time rates of change would be useful. The following factors are important for establishing a useful figure of merit:

1. Amplitude or phase step size or maximum rate of change between samples
2. Amplitude or phase error settling window
3. Sampling rate and number of samples averaged
4. Synchronization requirements

The relationship between these quantities could be evaluated and used in an expression to produce a numerical performance factor.

5.0 CONCLUSIONS

Results from this study show that instrumentation utilizing continuous time baseband filters or discrete time processes produce results with high precision when measuring a low rate of change signal. As expected, error levels do increase for both types of networks as the input signal rate of change becomes larger with respect to the aperture time or memory length. However, the DTP retains error levels approximately 10 dB lower than the LPF and BPF implementations for similar Equivalent Noise Bandwidths under all conditions. In many cases where continuous time lowpass filters are used to set the instrument's dynamic range, degradations in precision can be sufficient to require that data acquisition rates must be reduced substantially to facilitate acceptable settling. In systems where DTP techniques are utilized, the synchronized and fixed length signal memory provides precision only minimally impacted by high rate of change signals. This remains valid even when operating at the highest data acquisition speeds. The DTP technique, as used in the S-A 1795, allows data acquisition rates to be determined primarily by S/N considerations rather than by S/N and transient response considerations combined.

Additionally, instrumentation vendors should consider specification of impulse response instead of IF bandwidth as a figure of merit. Since the 3 dB bandwidth or the ENB of a measurement receiver's IF system is not necessarily an accurate representation of its total performance, this would allow users to perform their own error budgets based on expected signal dynamics.

6.0 COMPUTATIONS

Results from the modeling and simulations were calculated using the DaDISP signal processing program (version 1.05B) from DSP Development Corp., Cambridge, MA. Test cases showed errors due to floating point numeric representations of the quantities and the signal processing operations were less than -300 dB.

7.0 REFERENCES

- (1) O. M. Caldwell, "The Effects of Non-Systematic Errors on Measurement Uncertainty," 12th Meeting of the Antenna Measurement Techniques Association, October 9, 1990, Philadelphia, PA.
- (2) Charles M. Close, The Analysis of Linear Circuits. New York, N. Y. : Harcourt, Brace & World 1966
- (3) Y. T. Lo, and S. W. Lee, Antenna Handbook. New York, N. Y. : Van Nostrand Reinhold 1988
- (4) Ralph J. Schwarz and Bernard Friedland, Linear Systems. New York, N. Y. : McGraw-Hill 1965

FIGURE 1
RECEIVER SIGNAL PROCESSING
BLOCK DIAGRAM

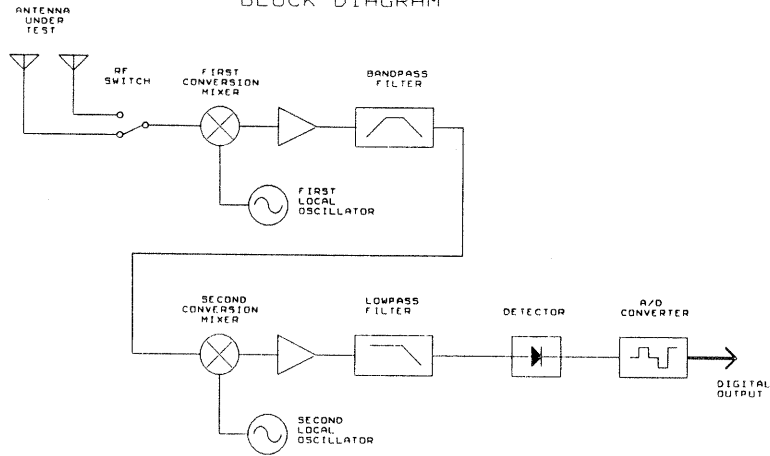


Figure 2 LPF

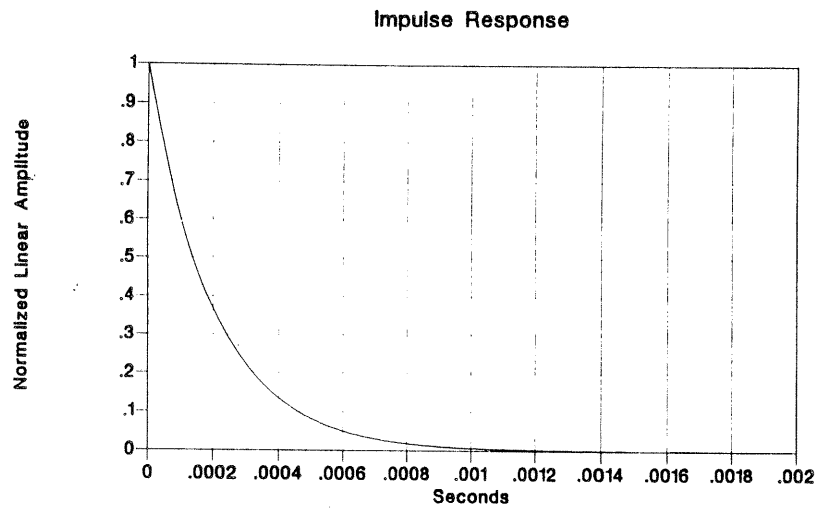
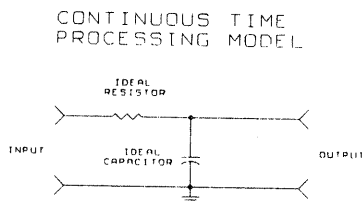


Figure 3 DTP

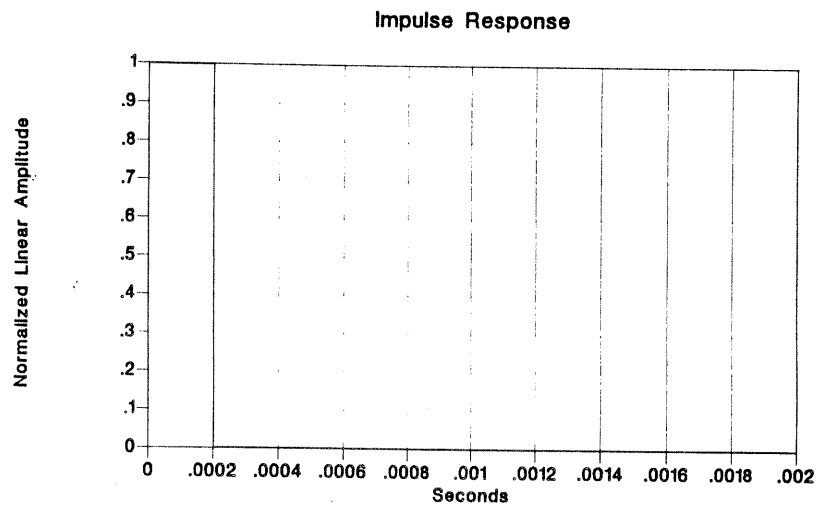
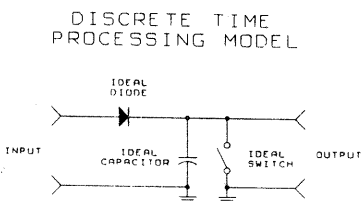


Figure 4
Ideal Copolarized Main Lobe

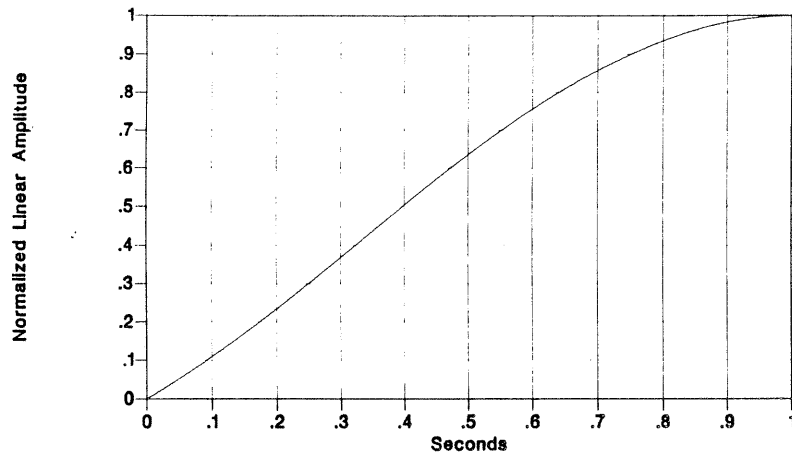


Figure 5
Error - Copolarized Main Lobe

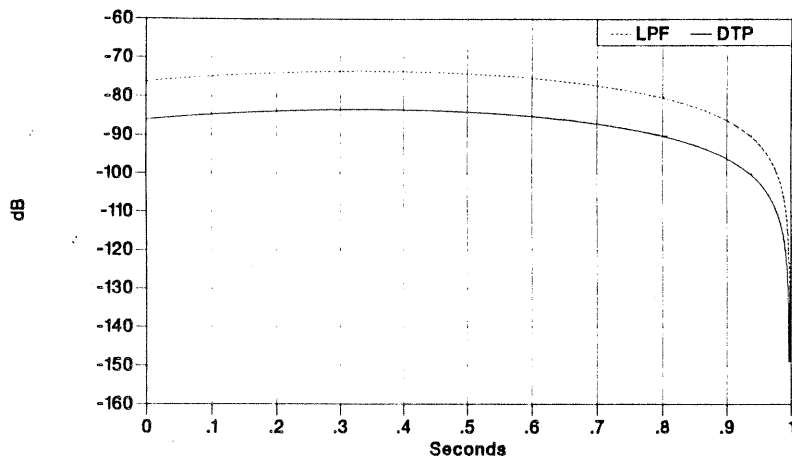


Figure 6
Spinning Polarization Pattern

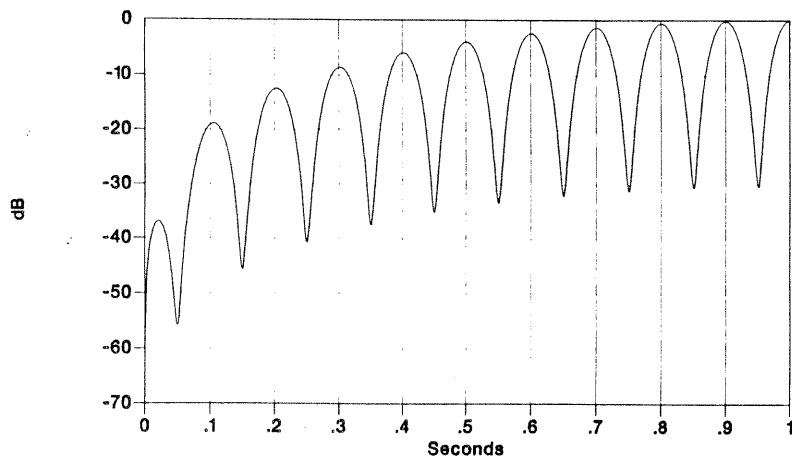


Figure 7
Error - Spinning Polarization Scan

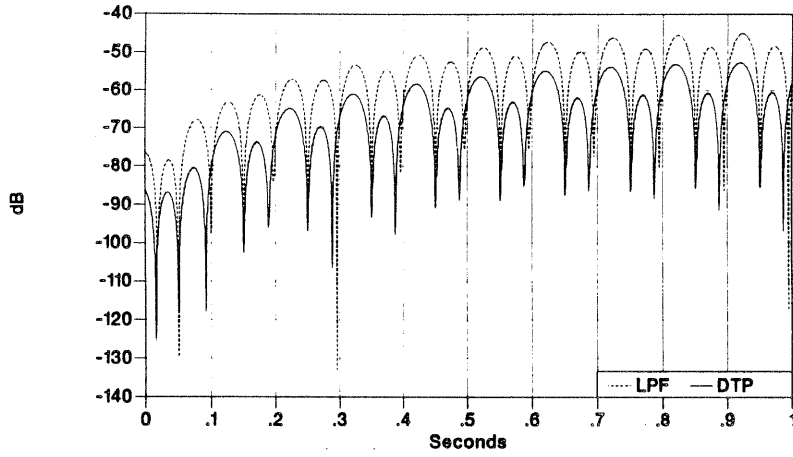


Figure 8
Switched Beam Excitation

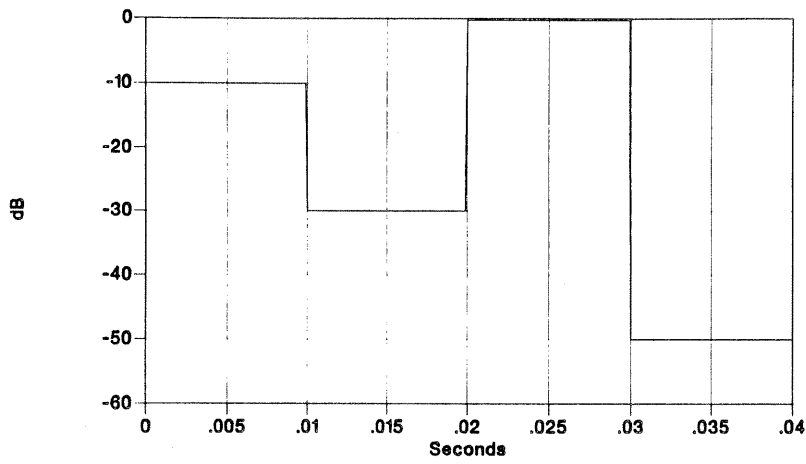


Figure 9
Error - Switched Beams

